

## RESEARCH ARTICLE

10.1002/2015JB011920

## Key Points:

- Cascadia Tremor and Slip associated with fluid release at fore-arc mantle corner
- Dehydrating subducting plate generates fluids
- Released fluids deposit quartz in the lower fore-arc crust

## Correspondence to:

R. D. Hyndman,  
rhyndman@nrcan.gc.ca

## Citation:

Hyndman, R. D., P. A. McCrory, A. Wech, H. Kao, and J. Ague (2015), Cascadia subducting plate fluids channelled to fore-arc mantle corner: ETS and silica deposition, *J. Geophys. Res. Solid Earth*, 120, 4344–4358, doi:10.1002/2015JB011920.

Received 29 JAN 2015

Accepted 10 MAY 2015

Accepted article online 14 MAY 2015

Published online 19 JUN 2015

## Cascadia subducting plate fluids channelled to fore-arc mantle corner: ETS and silica deposition

R. D. Hyndman<sup>1,2</sup>, P. A. McCrory<sup>3</sup>, A. Wech<sup>4</sup>, H. Kao<sup>1,2</sup>, and J. Ague<sup>5</sup>

<sup>1</sup>Pacific Geoscience Centre, Geological Survey of Canada, Sidney, British Columbia, Canada, <sup>2</sup>SEOS, University of Victoria, Victoria, British Columbia, Canada, <sup>3</sup>U.S. Geological Survey, Menlo Park, California, USA, <sup>4</sup>U.S. Geological Survey, Fairbanks, Alaska, USA, <sup>5</sup>Department of Geology and Geophysics, Yale University, New Haven, Connecticut, USA

**Abstract** In this study we first summarize the constraints that on the Cascadia subduction thrust, there is a 70 km gap downdip between the megathrust seismogenic zone and the Episodic Tremor and Slip (ETS) that lies further landward; there is not a continuous transition from unstable to conditionally stable sliding. Seismic rupture occurs mainly offshore for this hot subduction zone. ETS lies onshore. We then suggest what does control the downdip position of ETS. We conclude that fluids from dehydration of the downgoing plate, focused to rise above the fore-arc mantle corner, are responsible for ETS. There is a remarkable correspondence between the position of ETS and this corner along the whole margin. Hydrated mineral assemblages in the subducting oceanic crust and uppermost mantle are dehydrated with downdip increasing temperature, and seismic tomography data indicate that these fluids have strongly serpentinized the overlying fore-arc mantle. Laboratory data show that such fore-arc mantle serpentinite has low permeability and likely blocks vertical expulsion and restricts flow updip within the underlying permeable oceanic crust and subduction shear zone. At the fore-arc mantle corner these fluids are released upward into the more permeable overlying fore-arc crust. An indication of this fluid flux comes from low Poisson's Ratios (and  $V_p/V_s$ ) found above the corner that may be explained by a concentration of quartz which has exceptionally low Poisson's Ratio. The rising fluids should be silica saturated and precipitate quartz with decreasing temperature and pressure as they rise above the corner.

### 1. Introduction

Cascadia episodic tremor and slip (ETS) (Figure 1) involves slow slip in a margin-parallel band on or just above the subduction thrust at a depth of 35–40 km over periods of up to several weeks and at intervals of the order of a year (Figure 2). The slip is associated with seismic tremor that, unlike earthquakes, does not have a sharp onset [e.g., Rogers and Dragert, 2003; Schwartz and Rokosky, 2007; Gombert *et al.*, 2010]. On some subduction zones, tremor and slow slip have been observed in restricted areas at shallower depths [e.g., Dixon *et al.*, 2014; Obara, 2011] but not as yet for Cascadia. The relation between the deep band of tremor and slip and the shallower areas of tremor and slip is an important question, but we deal only with the band of deep tremor and slip as seen in Cascadia. For Cascadia, ETS occurs in a nearly continuous band along the margin where the estimated temperatures on the thrust are approximately 500°C, much too hot for normal crustal subduction thrust seismic behavior [e.g., Hyndman and Wang, 1993]. This slow slip has been commonly and reasonably considered to be a continuous downdip extension of unstable seismic behavior to conditionally stable slow slip behavior, but a gap is now recognized. The processes involved in slow slip are still poorly understood (see discussion by Segall *et al.* [2010]). One possibility is that the initial slip induces dilatation that reduces the pore pressure and increases the shear strength, thus stabilizing the ongoing slip.

In this article we first discuss the evidence that on the Cascadia subduction thrust, ETS is not continuous downdip with the seismogenic zone. There is an intervening gap of some 70 km. Second, we present the evidence that ETS are associated with fluids rising at the fore-arc mantle corner (Figure 1). The dehydration fluids that are expelled from the underlying subducting plate are focused to rise at this corner. There is evidence for these rising fluids in silica deposition in the overlying fore-arc crust above the fore-arc mantle corner inferred from seismic tomography data.

### 2. The Downdip Seismogenic Limit

The downdip limit for Cascadia great earthquake rupture is now quite well constrained [e.g., Hyndman, 2013, and references therein]. The most important indicators are (1) the downdip location of the maximum

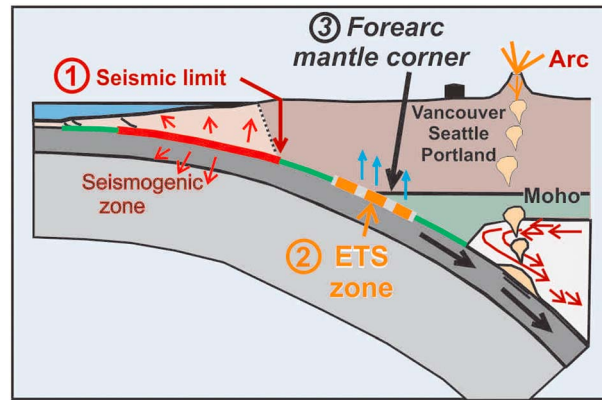


**Figure 1.** The locations of (1) the seismogenic zone downdip limit, (2) the tremor and slip, ETS zone, and (3) the fore-arc mantle corner.

temperature for seismic behavior; (2) the landward limit of the interseismic locked zone from dislocation models constrained by geodetic data, especially GPS, repeated leveling, and long-term tide gauge records; and (3) the coseismic subsidence as recorded in buried coastal marshes for the most recent great earthquake in 1700 and earlier great earthquakes. Although there are still significant uncertainties, these constraints and several others are in general agreement. The Cascadia downdip limit is concluded to be thermally limited to an unusually shallow depth because of the high temperatures resulting from the very young hot subducting plate [e.g., Hyndman and Wang, 1993]. Cascadia is an end-member subduction thrust with very few small thrust earthquakes [e.g., Williams et al., 2011; Obana et al., 2014], mainly ~M9, with perhaps smaller ~M8 events at south and north ends. For such subduction zones that are fully or nearly fully coupled, the downdip limit can be modeled by a seaward zone that is fully locked between great events and that has full rupture and a downdip tapering transition zone that extends to where there is no rupture displacement. Although there is undoubtedly variability among great events, this appears to be a good approximation to the long-term average [e.g., Leonard et al., 2010]. The corresponding interseismic period has a fully locked zone and a tapering zone downdip to where there is free slip or creep. The simplest form for the transition that fits the geodetic data well is a linear decrease in rupture displacement downdip as shown in Figure 3 [e.g., Hyndman and Wang, 1995]. This is a convenient reference model for comparison with the location of ETS. More sophisticated geodetic models and inversions that give a slightly better fit to the data have a smoother but similar transition [e.g., McCaffrey et al., 2007, 2013; Wang et al., 2003]. The modeled locked zones and the thrust rupture zones are similar but not identical because of postseismic transients [e.g., Wang et al., 2012]. For the likely material in the subduction thrust, laboratory data indicate a temperature limit for seismic

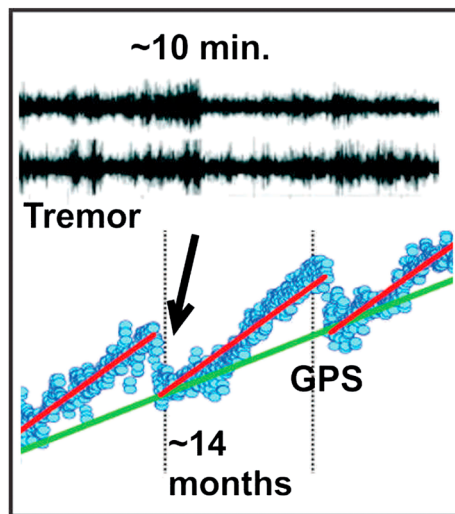


**Figure 2.** An example of episodic tremor and slip (ETS). The tremor is for a 10 min interval from the episode duration of several weeks. The GPS motion for a near-coastal station is generally landward for this locked subduction thrust, but during the slow slip of the ETS event, it moves seaward (adapted from Rogers and Dragert [2003]).

rupture initiation and full rupture of about 350°C, with a transition to zero displacement where the instantaneous shear strength becomes large at about 450°C. These limits agree with other constraints for the downdip rupture limit at several other hot subduction zones [e.g., Oleskevich et al., 1999; Hyndman et al., 1995; Currie et al., 2002]. For the Cascadia seismogenic zone, great earthquakes are concluded to accommodate most of the plate convergence, in contrast to many other subduction zones where some of the convergence is accommodated by aseismic motion. As yet there are no strong constraints for the updip seismic limit. Although not conclusive, for Cascadia it has been argued that, because of the unusually high temperatures on the updip portion of the thrust, stable-sliding clays are dehydrated at a shallow depth and rupture likely continues to near the deformation front [e.g., Hyndman and Wang, 1993; Hyndman, 2007]. This is in contrast to many other subduction zones that are cooler and have an updip aseismic zone. From these constraints, it is concluded that the downdip limit of the Cascadia seismogenic zone is almost all offshore. The modeled transition zone with significant displacement extends a short distance onshore only for northern Washington and northernmost California.

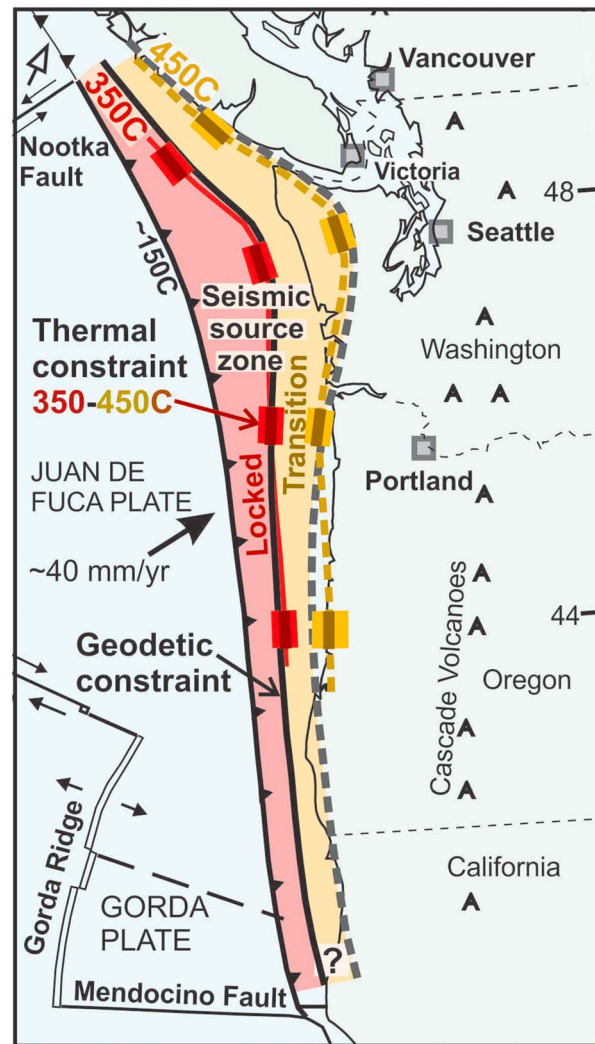


**Figure 3.** The downdip limit of the seismogenic zone, full rupture, and transition to zero rupture. The geodetic constraints are red and yellow shaded, and the thermal constraints on four profiles are shown by red, 350°C, and yellow, 450°C, rectangles. The landward limit of most rupture is seaward of the coast. The seaward limit of rupture is poorly constrained but in this model is assumed to extend to the deformation front (adapted from Hyndman [2013]).

In Figure 4a, we show the northern Cascadia location for one ETS event, with tremor from Kao *et al.* [2009] and slow slip location from Wang *et al.* [2008]. We also show a compilation of the locations of tremor for a number of events along the whole Cascadia margin (Figure 4b) from Wech [2010] and Wech and Creager [2008]. The volcanic arc is about 100 km further landward. There is some complexity in the nature of the tremor downdip [e.g., Wech and Creager, 2011; Audet and Bürgmann, 2014]. Szeliga *et al.* [2008], Schmidt and Gao [2010], and Schmalzle *et al.* [2014] show the locations of a series of slow slip events that correspond well to the compilation of tremor locations. The locations of the slip events again extend slightly seaward of the tremor. This discrepancy may reflect the difficulty of accurately defining the slip. If future analyses show the difference to be real, it is an important issue to be examined. For comparison, the figure also shows the megathrust locked and transition zones as shown in Figure 3. It is clear that the seismogenic zone and ETS slow slip zone do not overlap. There is about 70 km between the estimated 50% rupture average displacement (midtransition) and 50% of maximum slow slip displacement. The

### 3. The Location of ETS

Episodic tremor and slip (ETS) has been exceptionally well studied in Cascadia, along with SW Japan, the two areas where it was first observed clearly. ETS involves nonvolcanic seismic tremor with no clear onset [e.g., Rogers and Dragert, 2003; Schwartz and Rokosky, 2007; Gomberg *et al.*, 2010], that for much of Cascadia occurs variably but approximately at intervals of a year and lasts for several weeks. The tremor cannot be located as precisely as earthquakes which have sharp onsets, but several different methods give very similar locations. The depths have some uncertainty; some methods have it on or just above the subduction thrust [e.g., La Rocca *et al.*, 2009; Wech and Creager, 2007], and some methods yield a depth range extending somewhat shallower [e.g., Kao *et al.*, 2009]. The question of whether the tremor is on a sharp interface or distributed over some depth is important to the possible association of tremor with quartz vein deposition and is discussed below. There also are associated discrete Low-Frequency Earthquakes (LFEs) in the same area that appear to be restricted to a thin dipping zone on or near the top of the subducting oceanic crust. It has been suggested that the tremor may be composed of LFEs [e.g., Brown *et al.*, 2009].

Slow slip that occurs over several weeks at close to the same time interval as the tremor is also well characterized for Cascadia [e.g., Rogers and Dragert, 2003]. The slip is difficult to locate accurately, especially the depth, but inversions of geodetic data usually give locations that are very close to the tremor, although some slip may extend seaward of the tremor [e.g., Wech *et al.*, 2009; Schmidt and Gao, 2010].

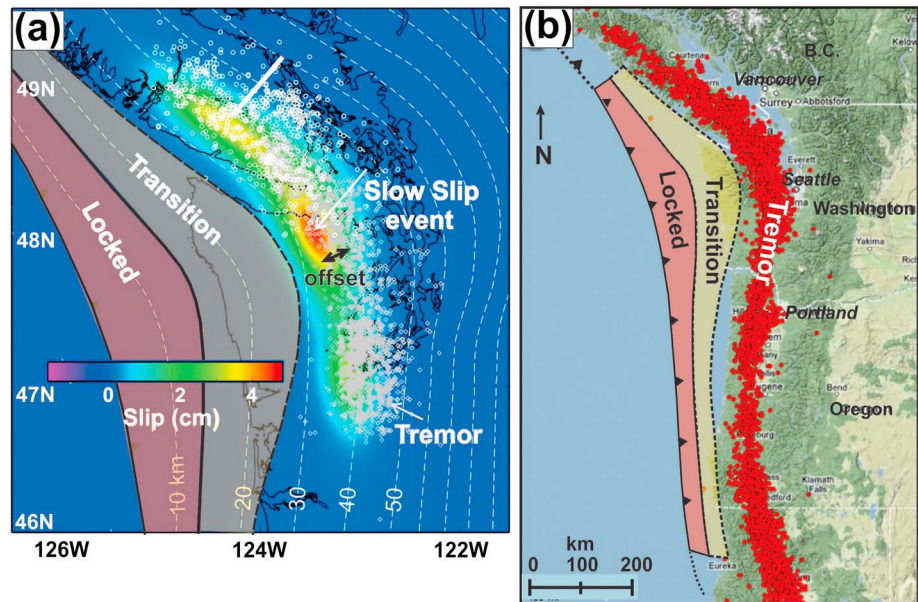


**Figure 4.** (a) Tremor for a single event in northern Cascadia (after Kao *et al.* [2009]), region of slow slip based on GPS data (after Wang *et al.* [2008]), and locked and transition seismogenic zones. (b) Compilation of tremor locations adapted from Wech [2010], compared to locked and transition seismogenic zone from Hyndman [2013].

separation has been indicated previously for several areas [e.g., Wech *et al.*, 2009; Hyndman, 2013]. Holtkamp and Brudzinski [2010] illustrate the separation in an inversion for the locked zones between both great earthquake and slow slip events (Figure 5). We show that there is a separation for the whole margin. This separation of the seismogenic zone from the zone of tremor also has been found vertically for the strike-slip San Andreas Fault [e.g., Shelly, 2010; Nadeau and Dolenc, 2005] and Alpine Fault in New Zealand [Wech *et al.*, 2012]. From magnetotelluric data across the San Andreas Fault, Becken *et al.* [2011] infer that deep fluids in the upper mantle stimulate the tremor and creep, and Kirby and Wang [2014] suggest that the overpressured fluids come from dehydration of the underlying former serpentinized fore-arc mantle that was cut off by the initiation of the fault.

The separation of the seismogenic zone and ETS zone on the Cascadia subduction thrust leaves us with the question, what does control the position of subduction zone ETS? Two other possibilities were examined by Peacock [2009]. Through comparison of several different subduction zones, he concluded that episodic tremor and slip do not coincide with a specific temperature or dehydration reaction. We conclude that the answer lies in the position of the fore-arc mantle corner, where the continental Moho reaches the downgoing plate and the rising fluids that are focused there.

#### 4. Fluid Expulsion From the Downgoing Plate Concentrated at Fore-Arc Mantle Corner

There have been a number of indications that ETS may be related to high fluid pressures above subducting plates. For example, Audet *et al.* [2009] and Peacock *et al.* [2011] inferred high Poisson's Ratio immediately above the Cascadia downgoing plate and attributed its origin to high pore pressure. Audet and Bürgmann [2014] concluded that slow slip is controlled by silica enrichment that modulates pore pressure on the thrust. Kodaira *et al.* [2004] suggested that the ETS slow slip for SW Japan is related to high fluid pressures. We provide here evidence that the fluid from the dehydrating oceanic plate is focused and concentrated into the crust over the fore-arc mantle corner and that this fluid is associated with ETS.

Subducting sediments, oceanic crust, and uppermost mantle contain large amounts of water in hydrated minerals that must be released with downdip increasing temperature and pressure [e.g., Ito *et al.*, 1983; Schmidt and Poli, 1998; Peacock, 1990; Hyndman and Peacock, 2003; Hacker *et al.*, 2003a; van Keken *et al.*, 2002, 2011].

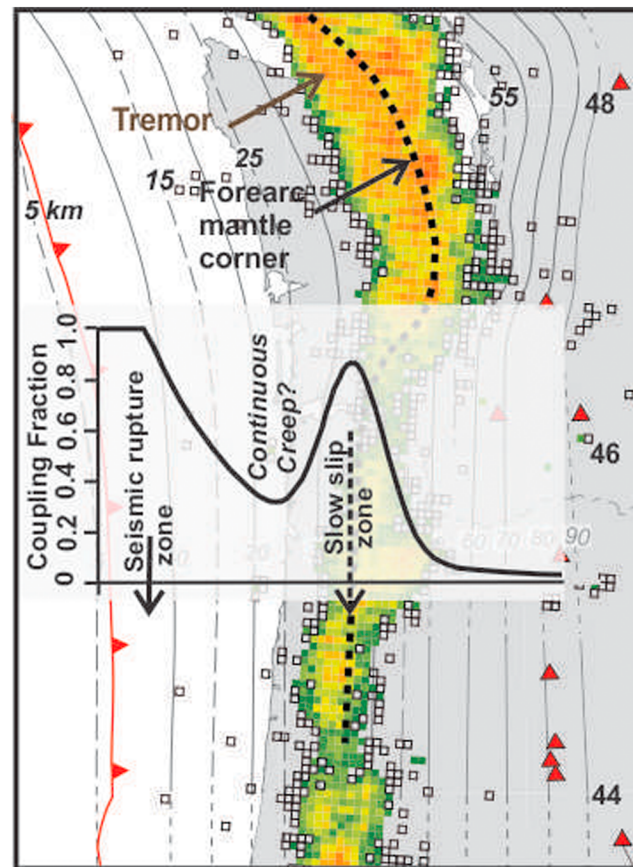


**Figure 5.** Inversion on a profile for seismogenic locked zone and ETS locked zone between events (after Holtkamp and Brudzinski [2010]), superimposed on map of the tremor and the fore-arc mantle corner (after McCrory *et al.* [2014a]), showing the excellent correspondence. The intervening zone on the thrust may exhibit longer-term creep. The contours are subduction thrust depths.

data [e.g., Carlson and Miller, 1997; Christensen, 1972], it may be significant based on ocean drilling results [e.g., Juteau *et al.*, 1990]. In addition to serpentinite formed at ridges and ocean basin fault zones, the upper mantle may be substantially serpentinitized at subduction zones by bending into the ocean trench. Rüpke *et al.* [2004] conclude that normal faulting occurring during plate bending between the outer rise and the trench axis provides fluid pathways for significant deepwater transport. Marine seismic reflection profiles in some areas show pronounced outer rise normal faults that cut into the mantle. The faults may act as conduits for seawater that result in extensive oceanic upper mantle serpentinitization. There is no evidence as yet for such outer rise serpentinitization for Cascadia, but in several studies of other subduction zones, uppermost mantle velocity reduction by hydration suggests 10–15% serpentinitization in the upper few kilometers of the mantle [Grevemeyer *et al.*, 2007; Ivandic *et al.*, 2008]. Ranero *et al.* [2003] and Worzewski *et al.* [2011] present the evidence for fluids penetrating the incoming plate mantle to form serpentinite at the Costa Rica margin from seismic velocity and magnetotelluric data. Scambelluria *et al.* [2004], Kendrick *et al.* [2011], and Angiboust *et al.* [2014] have discussed the dehydration at depth of this serpentinite. We suggest below that dehydration of a significant amount of serpentinite may be necessary for there to be enough fluid to explain the amounts of silica deposition inferred from seismic tomography data. As illustrated by Ague [2014], partially serpentinitized oceanic mantle may lose a large amount of water with dehydration at about 600°C, about 6 wt % water for his example. The amount of mantle dehydration water is poorly known, but it may significantly exceed that from the dehydrating oceanic crust [e.g., Schmidt and Poli, 1998, 2003]. The main dehydration temperature in the uppermost oceanic mantle of ~600°C is reached some tens of kilometers downdip of the fore-arc

Highly variable amounts of sediment are inferred to be subducted, that involve a substantial amount of porosity water. Most of the porosity should collapse and the fluid be expelled at shallow depth, although low-grade metamorphosed sediments may continue to a much greater depth. The upper crust has high porosity in both fracture and vesicular porosity, and there is substantial amount of water in hydrated mineral assemblages. At a depth where the temperature reaches 200–400°C, much of this water is released from basalt porosity collapse. At greater depths where the temperature reaches 400–500°C, much of the water in crustal hydrated mineral assemblages should be released. Although the breakdown temperatures and pressures are quite well known from laboratory studies, metastability and slow release mean that the depth of fluid release is not accurately known. The water production rate from the crust has been estimated to be about 0.1 mm/yr from these sources, near and just below the ETS zone for Cascadia [e.g., Peacock, 1990; Hyndman and Peacock, 2003].

A potentially larger but poorly constrained amount of water is contained in serpentinite in the incoming crust and upper mantle. Although the oceanic crust in the deep ocean basins has been concluded not to contain a large amount of serpentinite based on seismic velocity

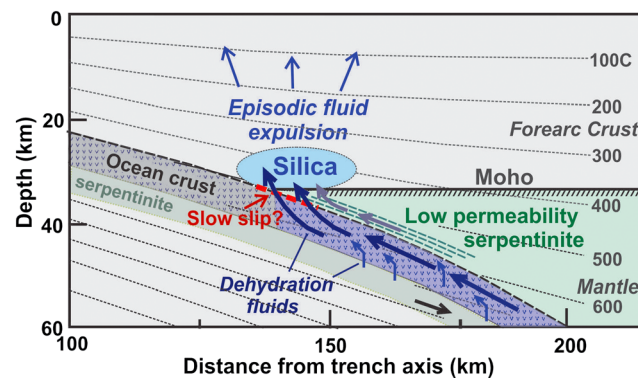


**Figure 6.** Model section showing updip fluid transport in permeable oceanic crust and subduction shear zone, under impermeable fore-arc mantle serpentinite. Silica deposition above the fore-arc mantle corner is inferred from seismic tomography data. Temperatures from Hyndman and Wang [1995].

Cascadia subduction zone. We expect that rising fluid from the dehydrating downgoing plate should hydrate the overlying fore-arc mantle, and seismic velocity data indicate that the overlying fore-arc mantle in Cascadia is strongly serpentinitized from these fluids [e.g., Zhao *et al.*, 2001; Bostock *et al.*, 2002; Brocher *et al.*, 2003; Carlson and Miller, 2003; Blakely *et al.*, 2005; Ramachandran and Hyndman, 2012]. The tomography Poisson's Ratios data discussed below allow semiquantitative estimates of the amounts of fluids. Mantle serpentinite also will be dehydrated at greater depths and expelled updip giving substantially more rising fluids.

## 5. Updip Fluid Channelling in Subducting Oceanic Crust

Recent laboratory data provide a reason why upward fluid expulsion should be concentrated at the fore-arc mantle corner. The laboratory studies indicate that the permeability of antigorite serpentinite as inferred for the fore-arc mantle should be very low [Katayama *et al.*, 2009; Kawano *et al.*, 2011; Okazaki *et al.*, 2013]. Fluid penetration from below into the fore-arc mantle also may be inhibited by the large increase in rock volume accompanying serpentinitization. In addition, these authors found that there is strong permeability anisotropy in the serpentinite, with higher permeability parallel to the shear so likely parallel to plate dip. Based on these data, Katayama *et al.* [2012] suggested that a contrast in permeability across the Moho results in the accumulation of water and the buildup of pore fluid pressure at the corner of the mantle wedge. Once the overlying fore-arc mantle is significantly hydrated, most of the rising fluid will be blocked from rising vertically by impermeable serpentinite. The fluid will be channelled updip in the subducting oceanic crust which has very high permeability [e.g., Fisher, 1998] or in the thrust zone itself that is often concluded to have high permeability parallel to the fault [e.g., Angiboust *et al.*, 2014]. Although the subducting ocean crustal permeability may be reduced by the progressive dehydration alteration process, the permeability is likely still much lower than the overlying serpentinitized fore-arc mantle. When the channelled fluids reach the fore-arc mantle corner they are no longer blocked by overlying impermeable serpentinite and may rise into the fore-arc crust.

As discussed by Ingebritsen and Manning [1999, 2002], fluids produced in the middle and lower continental crust may be transmitted to the upper crust through gabbro and other mafic rocks which they infer have quite high bulk permeability if there is high pore pressure. We therefore conclude that most of the dehydration fluid expelled from the subducting plate between the fore-arc mantle corner and the volcanic arc is channelled updip to be concentrated and rise into the overlying crust at the fore-arc mantle corner (Figure 6). Most previous estimates of rising fluid flux rates assumed that fluids rise vertically immediately above the dehydration location. Consideration of two factors results in potentially much larger estimates of the local focused fluid flux above the fore-arc mantle corner compared to previous regional estimates: (1) dehydration of the serpentinite in the incoming plate upper mantle in addition to ocean crustal dehydration and (2) focusing of rising fluids at the fore-arc mantle corner that were generated at greater depths and channelled updip in the subducting oceanic crust. Also, for our discussion of silica deposition

mantle corner. As discussed below, this water is expected to be channelled updip in the permeable oceanic crust and expelled upward mainly at or near the fore-arc mantle corner.

For hot subduction zones like Cascadia where a young hot oceanic plate is being underthrust, much of the crustal fluid is driven off at depths of 30–50 km. In contrast, for cold subduction zones much of the crustal dehydration occurs at a considerably greater depth, some of it beneath or landward of the volcanic arc [e.g., Peacock and Wang, 1999]. Especially large fluid expulsion is estimated between the fore-arc mantle corner and the arc for the very hot

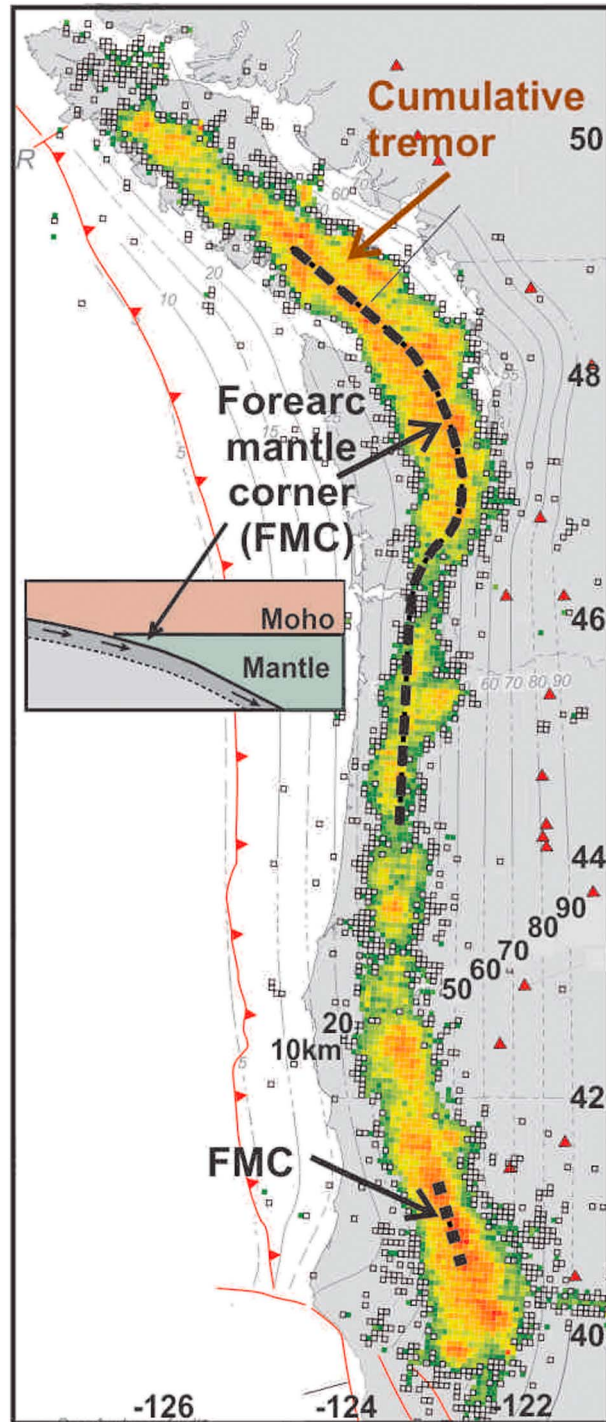


**Figure 7.** Map showing the Cascadia fore-arc mantle corner (after *McCroly et al.* [2014a]) (dashed line) with the addition of a new constraint in northern California, denoted by a dotted line (FMC). The yellow green dots are tremor with their intensity representing the density of the tremor occurrence. The gray lines are estimated depths to the top of the subducting oceanic plate, and the red triangles are active arc volcanoes.

location of ETS and the fore-arc mantle corner for the Cascadia margin, well within the location uncertainties. In Figure 7, we have added an important northernmost California location of the fore-arc mantle corner provided by the data of *Liu et al.* [2012]. As with the constraints further north, there is

above the corner, silica solubility will be much larger for dehydration fluids generated at greater depths and higher temperatures than at the ETS zone. Larger amounts of silica are therefore available to be released from the fluid with decreasing temperature, about a factor of 2 for 600°C compared to the 450–500°C on the thrust at the ETS zone. Some of this silica may precipitate during updip transport, but much may reach and be deposited above the fore-arc mantle corner. We conclude that upward fluid flux rates may as much as 5 to 10 times that for local oceanic crust and subducted sediment dehydration, i.e., ~1 mm/yr, but the uncertainties are very large.

## 6. The Location of the Fore-Arc Mantle Corner and Correspondence to ETS

A detailed review of constraining data and an analysis of the location of the Cascadia fore-arc mantle corner has recently been provided by *McCroly et al.* [2014a] (Figure 7). They constrained the corner location using published seismic structure data derived from wide-angle active source experiments, seismic tomography inversions of active source data, and receiver function transects from passive arrays recording distant earthquakes. Where available, they synthesized deep seismic velocity data to map the depth of the fore-arc Moho and its intersection with the dip profile of the subducting plate, the latter from an analysis of constraints by *McCroly et al.* [2012].

The subduction thrust is taken to be at the top of the subducting oceanic crust, but is recognized that there may be a subduction shear zone of some thickness above the top of the oceanic crust, especially downdip of where ductile behavior is reached. There are some alternative interpretations of the data, but the range of reasonable locations for the fore-arc mantle corner along most of the margin is quite small. *McCroly et al.* [2014a] demonstrate that there is a remarkable coincidence between the

excellent agreement between the tremor and this fore-arc mantle corner (FMC) location. This coincidence now recognized along the whole margin provides strong support for the conclusion discussed later in this article that ETS, both the tremor and the slow slip, is generated by fluids rising at the fore-arc mantle corner. A fluid origin of ETS also is in agreement with the evidence from magnetotelluric studies that there is an increase in electrical conductivity as the mantle wedge corner is approached, inferred to be due to a concentration of conductive fluid [Soyer and Unsworth, 2006; Wannamaker et al., 2014].

## 7. Low Poisson's Ratio in the Deep Fore-Arc Crust and Silica Deposition

Important evidence for fluids expelled upward at the fore-arc mantle corner comes from seismic velocities indicative of quartz deposited as the contained silica solubility decreases upward. Ramachandran and Hyndman [2012] provided seismic tomography data for the northern Cascadia subduction zone to a depth of about 60 km, approximately centered over the fore-arc mantle corner. Poisson's Ratios ( $\sigma$ ), which is directly related to  $V_p/V_s$ , is especially suited for defining regions of serpentinization and of quartz deposition both of which have unusual  $\sigma$  [e.g., Christensen, 1996]. The fore-arc section has a very uniform Poisson's Ratios,  $\sim 0.26$  ( $V_p/V_s \sim 1.76$ ), except for two anomalous regions. The fore-arc mantle near the corner has unusually high values of greater than 0.28. The only common rock type with such high Poisson's Ratios is serpentinite [e.g., Christensen, 1996], and this high value has been used by Ramachandran and Hyndman [2012] for a semiquantitative estimate of the degree of fore-arc mantle serpentinization, an average of about 30% for the 75 km landward of the corner.

The second anomalous region is an  $\sim 10$  km thick layer at the base of the deep fore-arc crust with Poisson's Ratios that is exceptionally low,  $\sigma$  less than 0.22 ( $V_p/V_s \sim 1.60$ ) (Figure 8) compared to regional values. This layer lies over the seaward limit of the fore-arc mantle wedge. The true horizontal extent may be somewhat less and the Poisson's Ratio even lower because many of the tomography raypaths are subhorizontal, such that the lateral extents are not well resolved. However, it is difficult to escape the conclusion that there is a lower crust region with exceptionally low Poisson's Ratios. These  $\sigma$  values are much lower than the tomography indicates for the rest of the fore-arc crust (see Figure 8), for the Cordillera to the east [e.g., Clowes et al., 1995], and for the common range of continental crustal values (e.g., the global compilation of Zandt and Ammon [1995]). The Poisson's Ratios of most of the fore-arc crust in these data is 0.26, which is within the range for common crustal rocks [Christensen, 1996].

Very few rocks have such low  $\sigma$ . The only common mineral with very low Poisson's Ratios is quartz, which is exceptionally low,  $\sigma \sim 0.1$  [Christensen, 1996], and we postulate high quartz concentrations to explain the observed low Poisson's Ratios. Using Poisson's Ratios of quartz ( $\sigma = 0.1$ ) and normal lower crust (0.26), the volume percent quartz estimated for an observed  $\sigma$  of  $\sim 0.22$  in this region is about 10%, assuming a nearly linear relation between Poisson's Ratios and quartz content as illustrated by Christensen [1996]. This amount is in addition to any quartz already contained in lower crustal rocks. There may be significant anisotropy either as horizontal sills, subvertical veins, or grain anisotropy, so this is only a semiquantitative estimate, with an uncertainty of at least a factor of 2. Significant silica-rich rocks are not normally expected in the lower continental crust, but they are expected in the special environment of the fore arc [e.g., Manning, 1996, 1997], and there is previous evidence in exposed former fore arcs [e.g., Breeding and Ague, 2002]. Audet and Bürgmann [2014] used the low  $\sigma$  from these data to argue for possible control of subduction zone slow earthquake periodicity by silica enrichment.

The indicator of rising fluid from the subducted plate, low Poisson's Ratios in the lowermost fore-arc crust, has large uncertainties with respect to the amount of silica deposition and in the required fluid amounts. However, the low Poisson's Ratios (and high  $V_s$ ) layer is well resolved and not easily explained as an artifact of the analysis, and silica deposition from rising fluids in the fore arc is expected. As explained below, our estimated amount of  $\sim 10\%$  silica requires greater upward fluid expulsion than that estimated for the  $\sim 40$  Myr current phase of subduction, assuming simple vertical flux solely from dehydrating oceanic crust. One explanation for the discrepancy is that the effect of silica on Poisson's Ratio may be larger than estimated because of anisotropy or other effect on seismic velocities. Probably, more important are the three other effects discussed below: dehydration of the serpentinite in the upper mantle of the incoming oceanic plate, focusing of rising fluids at the fore-arc mantle corner that were generated at greater depths,

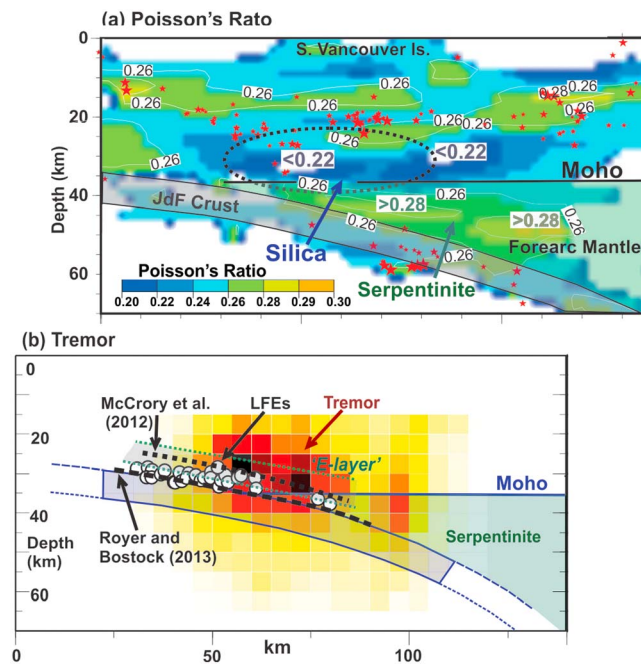


**Figure 8.** (b) Comparison of the distribution of tremor (after Kao *et al.* [2009]) and low-frequency earthquakes (LFEs) (after Royer and Bostock [2013]). The shaded dipping band is the inferred shear zone, seismic reflection “E” zone. (a) Seismic tomography (after Ramachandran and Hyndman [2012]) definition of high Poisson's Ratios in the fore-arc mantle (serpentinite) and low ratio in the fore-arc crust over the fore-arc mantle corner (silica). Note that the line projections are not identical so there may be small horizontal offsets for the different data.

and the greater silica solubility for fluids coming from greater depths where there are higher temperatures. All of these factors will increase the silica estimate substantially, although the total remains very uncertain.

The field observation of high concentrations of quartz veins in a similar position in an exposed deep subduction zone section by Breeding and Ague [2002] gives confidence that our interpretation is correct. Following Breeding and Ague [2002], we point out that the addition of a silica-rich layer will play a role in the overall composition of the continental crust. It usually has been assumed that the mafic arc volcanic rocks are the primary accretion material that extends the volume of continental crust. However, McLennan and Taylor [1996] have argued that the average continental crust could not have achieved its current high average silica content through magmatic differentiation of such rocks. If our estimate of silica deposited is correct and is applicable to many fore arcs, it represents a significant addition of silica to the lowermost crust making the accreted crust more felsic.

We have focused on Cascadia which is subducting a hot, young lithosphere. A similar process of quartz deposition is expected for the hot subduction zones such as SW Japan and Mexico. Subduction zones with older and faster incoming oceanic plates are colder, and much of the water must be dehydrated and released at greater depths. There may be less water released into the fore arc and more into the arc and back arc. Therefore, serpentinization of the fore-arc mantle may be slower and the formation of lower crust silica slower for older and therefore colder incoming plates.

## 8. Deposition of Silica From Rising Fluids Above the Fore-Arc Mantle Corner

An important characteristic of fluids dehydrated from metamorphic assemblages in the downgoing oceanic crust is that they should be silica (quartz) saturated. Metamorphosed silts and sands such as in the Cascadia accretionary prism usually contain quartz, and fluids in equilibrium with these rocks will be quartz saturated [e.g., Manning, 1996]. Whereas most mid-ocean ridge basalts are olivine normative, metamorphosed basalts commonly contain modal quartz coexisting with low-silica minerals such as chlorite [e.g., Peacock, 1993]. Aqueous fluids in equilibrium with oceanic crust metamorphosed to blueschist-facies assemblages thus will be saturated with respect to quartz. Peacock and Hyndman [1999] pointed out that the silica-rich fluids should result in deposition of talc along the subduction thrust beneath the fore-arc serpentinite. They conclude that this low-strength mineral provides an explanation for why the seismogenic zone for cool subduction zones commonly terminates downdip near the fore-arc mantle corner.

Silica saturation decreases rapidly with upward decreasing temperature, and pressure in the rising fluids so much of the dissolved silica will be deposited. For example, above the fore-arc mantle corner a decrease in temperature of 100°C from 500 to 400°C decreases the saturation by a factor of 3 and deposition of much of the dissolved silica as quartz veins [e.g., Manning, 1994, 1997]. For the fluids generated by dehydration reactions downdip at greater depth and higher temperatures, the silica saturation will be much greater,

more than twice as great at 600°C as it is at 500°C. These 600°C fluids therefore will hold much more silica in solution that will be precipitated as the fluid temperatures cool moving updip. These fluids generated at depths greater than the ETS zone may deposit some silica in transit updip in the permeable oceanic crust, but two processes may limit this deposition: (1) the kinetic effect limiting silica release if the fluid movement is rapid, i.e., the “overstepping” effect of a few degrees to as much as 80°C [e.g., *Ague et al.*, 1998] or rapid ascent of the fluids in mobile hydrofractures, i.e., fractures that open ahead of a packet of fluid and close behind it [*Bons*, 2001]. The temperature gradients are much more gradual for the fluid moving updip in the permeable oceanic crust compared to the much steeper vertical gradients above the fore-arc mantle corner. The pressure decrease also is much greater vertically above the fore-arc mantle corner than for the fluid moving updip in the permeable oceanic crust. A rapid pressure drop of the fluids rising above the fore-arc mantle corner as well as the temperature reduction may release much of the silica.

In a relevant study, quartz deposited in the now exposed deep fore arc from silica-rich fluids interpreted as rising from the subducted slab was described by *Breeding and Ague* [2002]. Their study was for outcrop of the landward part of a former very thick accretionary sedimentary prism in New Zealand where the depth of deposition and greenschist-facies *P-T* conditions of 350–450°C and 600–800 MPa (6–8 kbar) are similar but slightly cooler than the region of the Cascadia fore-arc mantle corner of about 500°C [e.g., *Hyndman and Wang*, 1995; *Hacker et al.*, 2003a, 2003b]. *Breeding and Ague* [2002] estimated 4% mass increase from quartz veins in their deep section, a similar order but somewhat lower than the ~10% that appears to be required to explain the observed low Poisson's Ratios in Cascadia. They showed that the observed amounts of quartz veins represented approximately the amount of silica expected to be deposited in the fore arc from the ~100 Myr of subduction inferred for that area.

We have estimated the time required to form a 10% concentration of silica in the lower fore-arc crust. The calculation method is given by *Breeding and Ague* [2002] and more details by *Philpotts and Ague* [2009, pp. 530–532]. Using a vertical fluid expulsion rate of about 0.1 mm/yr from oceanic crust dehydration only, approximately 400 Myr is required. It has been appreciated that this is much longer than the current ~40 Myr phase of Cascadia subduction [e.g., *Ramachandran and Hyndman*, 2012; *Peacock*, 1993], i.e., a fluid expulsion rate that is a factor of 10 too small. However, we now have several newly recognized factors that give much larger estimates of fluid expulsion at the fore-arc mantle corner and that could resolve this discrepancy: (1) downgoing plate dehydration fluids may be channelled updip to the corner from considerable depth, perhaps from as far as the overlying volcanic arc; (2) substantial water may be contained in the incoming oceanic upper mantle serpentinite, especially incorporated from bending fracturing just seaward of the subduction trench; and (3) fluids from depths well below the fore-arc mantle corner will be generated at high temperatures at least 600°C where the solubility of silica is very high, especially fluids from dehydration of oceanic upper mantle serpentinite. With a large uncertainty, these effects may result in total focused fluid expulsion at the fore-arc mantle corner of up to 1 mm/yr, i.e., 10 times the simple local vertical rate, as required for the estimated amount of silica.

A question that needs further study is the silica content of fluids produced by dehydration of ocean plate upper mantle serpentinite. Ultramafic rocks are undersaturated with respect to silica so serpentinite dehydration may not produce silica-saturated fluid. However, some serpentinite dehydration reactions may release silica, and the fluids may react and equilibrate with the overlying oceanic crust before reaching the fore-arc mantle corner. Finally, even a fluid that is undersaturated with respect to silica at the higher temperatures at greater depths could become significantly supersaturated as it migrates to shallower depths.

A portion of the rising dehydration fluid goes into serpentinitization of the fore-arc mantle wedge. This fluid is not available to produce silica at the fore-arc mantle corner. However, as shown by *Ramachandran and Hyndman* [2012], a vertically rising rate of 0.1 mm/yr local expulsion total is enough to generate the estimated serpentinitization, so this is not a large factor if the expulsion at the fore-arc mantle corner is 10 times larger. Also, the main upward fluid flux is above the corner of the fore-arc mantle wedge where the fore-arc mantle section is thin. As described by *Manning* [1997] and *Peacock* [1993], substantial silica should be removed from such rising fluids by conversion of any brucite present to serpentinite and then formation of talc. *McCroly et al.* [2014b] provide evidence from helium isotopes that some slab-derived fluids reach surface hot springs at and landward of the fore-arc mantle corner. A quite high Poisson's Ratios

occurs near the tip of the fore-arc mantle corner in the area of the tomography study. This could be due to high pore pressure [Peacock *et al.*, 2011]. We also note that above about 600°C antigorite serpentinite is not stable so deeper fluids may transit updip unaltered.

## 9. Quartz Vein Formation and Tremor

An important question that follows from our study is the relation between quartz vein formation and ETS tremor. Some observations suggest that they may be closely related. A model proposed by Audet and Bürgmann [2014] is that silica enrichment controls ETS slow slip. Are the tremors produced by very rapid formation of quartz veins that also involve displacement? From a number of detailed studies of quartz veins it has been concluded that the veins are generated as multiple layers from fluid transport in very rapid short intervals, perhaps with opening near the fracture velocity. Crack seal deformation could heal slip events through dilatancy that stabilizes slow slip instabilities [e.g., Segall *et al.*, 2010]. Slow slip may involve a process related to the fault valve model of earthquakes [e.g., Sibson, 1992] with silica deposition temporarily blocking fluid flow. A relevant study was by Birtel and Stöckhert [2008] of an exhumed section in Norway with extensive quartz veins. The formation temperature was 500–550°C at depths of 15–25 km, i.e., slightly shallower but at similar temperatures to the conditions for Cascadia ETS. They found that the veins formed in open large aspect fractures that cut across the host rocks foliation and structures. The veins therefore were formed by intense inhomogeneous ductile deformation of the host rock, not by simple high-pressure fluid hydrofracturing that tends to follow foliation and preexisting weaknesses. They suggested formation of the quartz veins at the time of seismic rupture on a nearby thrust fault. Although the temperature of vein formation of 500–550°C is too high for normal crustal seismic rupture, i.e., a maximum of about 350°C, low-frequency earthquakes, LFEs, do occur at these high temperatures.

It is tempting to associate the tremor of ETS with the formation of the quartz above the fore-arc mantle corner. However, there are several reasons why this is unlikely. First, quartz veins and the associated fluid transport events would need to be of the dimensions required to produce the estimated magnitudes of tremor. Also, the fluid transport events would need to be associated with slip displacement to produce the inferred double-couple signals of low-frequency earthquakes. These questions need further study. Second, although not yet conclusive, there is increasing evidence that most of the tremor is associated with low-frequency earthquakes that occur on a dipping plane at or near the top of the subducting plate. If the low Poisson's Ratio zone is associated with quartz deposition and the tremor is associated with quartz vein formation, we expect the tremor to have a considerable vertical extent. Several analysis methods have given a tremor vertical extent of 5–10 km [e.g., Kao *et al.*, 2009]. Kao *et al.* also concluded that the tremor was spatially correlated to the E-zone reflectors in that area [e.g., Clowes *et al.*, 1987] that may define the subduction shear zone [Nedimović *et al.*, 2003] (dashed green lines in Figure 8). We carried out a new routine, updated from Kao *et al.* [2009], for defining the tremor locations. The routine selects only those tremors with nearby events. Isolated tremors are excluded. This approach gives a narrower depth range for the majority of events (Figure 8). There is better correspondence between the tremor and the top of the oceanic plate based on new data by Royer and Bostock [2013] than with the previous estimates summarized by McCrory *et al.* [2012]. Note that the sections shown are where there is a corner in the margin so there is not an exact relative positions for tremor, Poisson's Ratio, and the E zone.

This 5–10 km thick distribution also is consistent with inferences from dipping reflectors in multichannel seismic reflection data above the subducting oceanic crust of a thick shear zone in the ductile regime where tremor commonly occurs [e.g., Nedimović *et al.*, 2003]. Thick shear zones also are often found in paleosubduction thrusts [e.g., Fagereng, 2011; Cloos and Shreve, 1988]. The depth to the top of the subducting oceanic plate has been debated for some time. In Figure 8, we show the depth estimated from the depths of low-frequency earthquakes (LFEs) associated with tremor [Royer and Bostock, 2013]. Other analyses of the depth of tremor indicate a thin dipping zone at or near the subduction thrust, and the associated low-frequency earthquakes (LFEs) have been located on a thin band with rupture mechanisms that correspond to the thrust dip angle [e.g., Shelly *et al.*, 2007; Ide *et al.*, 2007; Armbruster *et al.*, 2014]. The association of ETS and quartz deposition from dehydration fluids rising updip in the subducting oceanic crust is an important subject for further study. The quartz above the thrust may be associated but not directly related.

## 10. Conclusions

We have shown that ETS is separated from the Cascadia seismogenic zone by a downdip gap of ~70 km. This gap is consistent with the vertical gap between normal seismicity and tremor in the near-vertical San Andreas Fault in California and the Alpine Fault of New Zealand. There is not a continuous downdip change on the subduction thrust from seismic unstable behavior to conditional stability of slow slip. Another explanation is required for the downdip position of ETS.

There is a very close spatial correspondence between tremor and slow slip (ETS) and the fore-arc mantle corner along the length of the Cascadia margin. This association can be explained by high fluid flow and pressures developing at the fore-arc mantle corner. Fluids from dehydration of the downgoing plate below the fore-arc mantle are blocked from moving vertically upward by low-permeability serpentinized fore-arc mantle. Fluid transport is channelled updip in the permeable subducting oceanic crust and subduction shear zone until it reaches the fore-arc mantle corner, where it is expelled upward into the overlying fore-arc crust in the region of ETS.

Rising ocean plate dehydration fluids should be silica saturated, and substantial deposition of silica is expected as the fluids move upward above the fore-arc mantle corner, since silica saturation decreases rapidly with upward decreasing temperature and pressure. Substantial concentrations of quartz are therefore expected above the dehydrating subducting oceanic plate, especially over the fore-arc mantle corner. Unusually, low Poisson's Ratios occur in the fore-arc crust in the region over the fore-arc mantle corner based on seismic tomography data. Even with the considerable uncertainties in the details of the tomography anomaly, these data clearly delineate an area of unusually low Poisson's Ratio. Quartz has exceptionally low Poisson's Ratios and seems the only reasonable source of this anomaly. The deposition of the estimated ~10% silica requires a very large amounts of water. Local vertical flux from the oceanic crust as it progressively dehydrates downdip over the 40 Myr of the most recent phase of subduction can account for only ~10% of the fluid needed. However, three newly recognized factors make the estimated total fluids closer to those required for the estimated silica amounts: dehydration of the serpentinite in the upper mantle of the incoming oceanic plate, focusing of rising fluids at the fore-arc mantle corner that were generated at greater depths, and the greater silica solubility for fluids coming from greater depths where there are higher temperatures.

An important question that follows from our study is the relation between quartz vein formation and ETS tremor. Are the tremor produced by very rapid formation such as crack seal, of quartz veins? From a number of detailed studies it has been concluded that most quartz veins are generated as multiple layers from fluid transport in very rapid short intervals, perhaps with opening near the fracture velocity [e.g., *Birtel and Stöckhert*, 2008]. Are the ETS tremors generated by these quartz vein formation events with associated small displacements? If so, can vein formation events for the ETS tremor be reconciled with the seismic constraints on tremor polarization and the mechanisms of low-frequency earthquakes on a thin dipping plane?

We finish by noting several speculations on the importance of the large amounts of fluid being expelled into the crust above the fore-arc mantle corner. The first, as noted earlier, is the accumulating global amount of silica input into the crust from this source, for global average crustal compositions [e.g., *McLennan and Taylor*, 1996]. The second is the possible role of these fluids in the formation of the very common quartz veins in outcrop sections, especially where there are high concentrations of veins in metamorphic terranes. Very large amounts of fluid are required since the solubility of quartz is quite small, especially at shallow depths. We are not aware that a sufficient fluid source has previously been identified [see *Jia and Kerrich*, 2000; *Jia et al.*, 2003; *Bons*, 2001]. Finally, there is a possible role of these focused fluids in the formation of mesothermal gold, often associated with quartz veins. Solution of gold in the deep source region and subsequent deposition involve complex chemistry, but huge amounts of fluid are usually inferred to be required through the source and deposition regions [see *Phillips and Powell*, 2010]. The fore-arc mantle corner focused fluid is one possible source.

### Acknowledgments

The authors wish to acknowledge discussions with numerous scientists that led to this article. The various data used in this article all come from articles given in the reference list.

### References

- Ague, J. J. (2014), Fluid flow in the deep crust, in *Treatise on Geochemistry*, 2nd ed., vol. 4, edited by H. D. Holland and K. K. Turekian, pp. 203–247, Elsevier, Oxford.
- Ague, J. J., J. Park, and D. M. Rye (1998), Regional metamorphic dehydration and seismic hazard, *Geophys. Res. Lett.*, *25*, 4221–4224, doi:10.1029/1998GL900124.
- Angiboust, S., T. Pettke, J. C. M. De Hoog, B. Caron, and O. Oncken (2014), Channelized fluid flow and eclogite-facies metasomatism along the subduction shear zone, *J. Petrol.*, *55*, 883–916, doi:10.1093/petrology/egu010.

- Armbruster, J. G., W. Y. Kim, and A. M. Rubin (2014), Accurate tremor locations from coherent *S* and *P* waves, *J. Geophys. Res. Solid Earth*, *119*, 5000–5013, doi:10.1002/2014JB011133.
- Audet, P., and R. Bürgmann (2014), Possible control of subduction zone slow-earthquake periodicity by silica enrichment, *Nature*, *510*, 389–392, doi:10.1038/nature13391.
- Audet, P., M. G. Bostock, N. I. Christensen, and S. M. Peacock (2009), Seismic evidence for overpressured subducted oceanic crust and megathrust fault sealing, *Nature*, *457*, 76–78.
- Becken, M., O. Ritter, P. A. Bedrosian, and U. Weckmann (2011), Correlation between deep fluids, tremor and creep along the central San Andreas Fault, *Nature*, *480*, 87–90, doi:10.1038/nature10609.
- Birtel, S., and B. Stöckhert (2008), Quartz veins record earthquake-related brittle failure and short term ductile flow in the deep crust, *Tectonophysics*, *457*, 53–63, doi:10.1016/j.tecto.2008.05018.
- Blakely, R. J., T. M. Brocher, and R. E. Wells (2005), Subduction zone magnetic anomalies and implications for hydrated forearc mantle, *Geology*, *33*, 445–448, doi:10.1130/G21447.1.
- Bons, P. D. (2001), The formation of large quartz veins by rapid ascent of fluids in mobile hydrofractures, *Tectonophysics*, *336*, 1–17.
- Bostock, M. G., R. D. Hyndman, S. Rondenay, and S. M. Peacock (2002), An inverted continental Moho and the serpentinization of the forearc mantle, *Nature*, *417*, 536–538.
- Breeding, C. M., and J. J. Ague (2002), Slab-derived fluids and quartz-vein formation in an accretionary prism, Otago Schist, New Zealand, *Geology*, *30*, 499–502.
- Brocher, T. M., T. Parsons, A. M. Trehu, C. M. Snelson, and M. A. Fisher (2003), Seismic evidence for widespread serpentinized forearc upper mantle along the Cascadia margin, *Geology*, *31*, 267–270.
- Brown, J. R., G. C. Beroza, S. Ide, K. Ohta, D. R. Shelly, S. Y. Schwartz, W. Rabbel, M. Thorwart, and H. Kao (2009), Deep low-frequency earthquakes in tremor localize to the plate interface in multiple subduction zones, *Geophys. Res. Lett.*, *36*, L19306, doi:10.1029/2009GL040027.
- Carlson, R. L., and D. J. Miller (1997), A new assessment of the abundance of serpentinite in the oceanic crust, *Geophys. Res. Lett.*, *24*, 457–460, doi:10.1029/97GL00144.
- Carlson, R. L., and D. J. Miller (2003), Mantle wedge water contents estimated from seismic velocities in partially serpentinized peridotites, *Geophys. Res. Lett.*, *30*(5), 1250, doi:10.1029/2002GL016600.
- Christensen, N. I. (1972), The abundance of serpentinites in the oceanic crust, *J. Geol.*, *80*, 709–719.
- Christensen, N. I. (1996), Poisson's Ratios and crustal seismology, *J. Geophys. Res.*, *101*, 3139–3156, doi:10.1029/95JB03446.
- Cloos, M., and R. L. Shreve (1988), Subduction-channel model of prism accretion, melange formation, sediment subduction, and subduction erosion at convergent plate margins: 2. Implications and discussion, *Pure Appl. Geophys.*, *128*, 501–545.
- Clowes, R. M., M. T. Brandon, A. G. Green, C. J. Yorath, A. Sutherland Brown, E. R. Kanasevich, and C. Spencer (1987), LITHOPROBE-southern Vancouver Island: Cenozoic subduction complex imaged by deep seismic reflections, *Can. J. Earth Sci.*, *24*, 31–51.
- Clowes, R. M., C. A. Zelt, J. R. Amor, and R. M. Ellis (1995), Lithospheric structure in the southern Canadian Cordillera from a network of seismic refraction lines, *Can. J. Earth Sci.*, *32*, 1485–1513.
- Currie, C. A., R. D. Hyndman, K. Wang, and V. Kostoglodov (2002), Thermal models of the Mexico subduction zone: Implications for the megathrust seismogenic zone, *J. Geophys. Res.*, *107*(B12), 2370, doi:10.1029/2001JB000886.
- Dixon, T. H., Y. Jiang, R. Malservisia, R. McCaffrey, N. Vossa, M. Protti, and V. Gonzalez (2014), Earthquake and tsunami forecasts: Relation of slow slip events to subsequent earthquake rupture, *Proc. Natl. Acad. Sci. U.S.A.*, *111*, 17,039–17,044, doi:10.1073/pnas.1412299111.
- Fagereng, Å. (2011), Geology of the seismogenic subduction thrust interface, *Geol. Soc. London, Spec. Publ.*, *359*, 55–76.
- Fisher, A. T. (1998), Permeability within basaltic oceanic crust, *Rev. Geophys.*, *36*, 143–182, doi:10.1029/97RG02916.
- Gomberg, J., et al. (2010), Slow-slip phenomena in Cascadia from 2007 and beyond: A review, *Geol. Soc. Am. Bull.*, *122*, 963–978, doi:10.1130/B30287.1.
- Grevemeyer, I. C. R., E. R. Ranero, D. K. Flueh, and J. Bialas (2007), Passive and active seismological study of bending-related faulting and mantle serpentinization at the Middle America trench, *Earth Planet. Sci. Lett.*, *258*, 528–542.
- Hacker, B. R., G. A. Abers, and S. M. Peacock (2003a), Subduction factory 1. Theoretical mineralogy, densities, seismic wave speeds, and H<sub>2</sub>O contents, *J. Geophys. Res.*, *108*(B1), 2029, doi:10.1029/2001JB001127.
- Hacker, B. R., S. M. Peacock, G. A. Abers, and S. D. Holloway (2003b), Subduction factory 2. Are intermediate-depth earthquakes in subducting slabs linked to metamorphic dehydration reactions?, *J. Geophys. Res.*, *108*(B1), 2030, doi:10.1029/2001JB001129.
- Holtkamp, S., and M. R. Brudzinski (2010), Determination of slow slip episodes and strain accumulation along the Cascadia margin, *J. Geophys. Res.*, *115*, B00A17, doi:10.1029/2008JB006058.
- Hyndman, R. D. (2007), The seismogenic zone of subduction thrust faults: What we know and don't know, in *The Seismogenic Zone of Subduction Thrust Faults*, edited by T. Dixon, pp. 15–49, Columbia Univ. Press, New York.
- Hyndman, R. D. (2013), Downdip landward limit of Cascadia great earthquake rupture, *J. Geophys. Res. Solid Earth*, *118*, 5,530–5,549, doi:10.1002/jgrb.50390.
- Hyndman, R. D., and S. M. Peacock (2003), Serpentinization of the forearc mantle, *Earth Planet. Sci. Lett.*, *212*, 417–432.
- Hyndman, R. D., and K. Wang (1993), Thermal constraints on the zone of major thrust earthquake failure: The Cascadia subduction zone, *J. Geophys. Res.*, *98*, 2039–2060, doi:10.1029/92JB02279.
- Hyndman, R. D., and K. Wang (1995), The rupture zone of Cascadia great earthquakes from current deformation and the thermal regime, *J. Geophys. Res.*, *100*, 22,133–22,154, doi:10.1029/95JB01970.
- Hyndman, R. D., K. Wang, and M. Yamano (1995), Thermal constraints on the seismogenic portion of the southwestern Japan subduction thrust, *J. Geophys. Res.*, *100*, 15,373–15,392, doi:10.1029/95JB00153.
- Ide, S., D. R. Shelly, and G. C. Beroza (2007), Mechanism of deep low frequency earthquakes: Further evidence that deep non-volcanic tremor is generated by shear slip on the plate interface, *Geophys. Res. Lett.*, *34*, L03308, doi:10.1029/2006GL028890.
- Ingebritsen, S. E., and C. E. Manning (1999), Geological implications of a permeability-depth curve for the continental crust, *Geology*, *27*, 1107–1110.
- Ingebritsen, S. E., and C. E. Manning (2002), Diffuse fluid flux through orogenic belts: Implications for the world ocean, *Proc. Natl. Acad. Sci. U.S.A.*, *99*, 9113–9116.
- Ito, E., D. M. Harris, and A. T. Anderson Jr. (1983), Alteration of oceanic crust and geologic cycling of chlorine and water, *Geochim. Cosmochim. Acta*, *47*(9), 1613–1624.
- Ivancic, M., I. Grevemeyer, A. Berhorst, E. R. Flueh, and K. McIntosh (2008), Impact of bending related faulting on the seismic properties of the incoming oceanic plate offshore of Nicaragua, *J. Geophys. Res.*, *113*, B05410, doi:10.1029/2007JB005291.
- Jia, Y., and R. Kerrich (2000), Giant quartz vein systems in accretionary orogenic belts: The evidence for a metamorphic fluid origin from  $\delta^{15}\text{C}$  and  $\delta^{13}\text{C}$  studies, *Earth Planet. Sci. Lett.*, *184*, 211–224.

- Jia, Y., R. Kerrich, and R. Goldfarb (2003), Metamorphic origin of ore-forming fluids for orogenic gold-bearing quartz vein systems in the North American Cordillera: Constraints from a reconnaissance study of  $\delta^{15}\text{N}$ ,  $\delta\text{D}$ , and  $\delta^{18}\text{O}$ , *Econ. Geol.*, *98*, 109–123.
- Juteau, T., M. Cannat, and Y. Lagabriele (1990), Serpentinized peridotites in the upper oceanic crust away from transform zones: A comparison of the results of previous DSDP and ODP legs, *Proc. ODP, Sci. Results*, *106*, 303–312.
- Kao, H., S.-J. Shan, H. Dragert, and G. C. Rogers (2009), Northern Cascadia episodic tremor and slip: A decade of tremor observations from 1997 to 2007, *J. Geophys. Res.*, *114*, B00A12, doi:10.1029/2008JB006046.
- Katayama, I., K. Hirauchi, K. Michibayashi, and J. I. Ando (2009), Trench-parallel anisotropy produced by serpentine deformation in the hydrated mantle wedge, *Nature*, *461*, 1114–1117.
- Katayama, I., T. Terada, K. Okazaki, and W. Tanikawa (2012), Episodic tremor and slow slip potentially linked to permeability contrasts at the Moho, *Nat. Geosci.*, *5*, 731–734.
- Kawano, S., I. Katayama, and K. Okazaki (2011), Permeability anisotropy of serpentinite and fluid pathways in a subduction zone, *Geology*, *39*, 939–942.
- Kendrick, M. A., M. Scambelluri, M. Honda, and D. Phillips (2011), High abundances of noble gas and chlorine delivered to the mantle by serpentinite subduction, *Nat. Geosci.*, *4*, 807–812.
- Kirby, S. K., and T. B. Wang (2014), A possible deep, long-term source for water in the northern San Andreas Fault system: A ghost of Cascadia subduction past?, *Earth Planets Space*, *66*, 1–18.
- Kodaira, S., T. Iidaka, A. Kato, J. O. Park, T. Iwasaki, and Y. Kaneda (2004), High pore fluid pressure may cause silent slip in the Nankai Trough, *Science*, *304*, 1295–1298.
- La Rocca, M., K. C. Creager, D. Galluzzo, S. Malone, J. E. Vidale, J. R. Sweet, and A. G. Wech (2009), Cascadia tremor located near plate interface constrained by  $S$  minus  $P$  wave times, *Science*, *323*, 620–623.
- Leonard, L. J., C. A. Currie, S. Mazzotti, and R. D. Hyndman (2010), Rupture area and displacement of past Cascadia great earthquakes from coastal coseismic subsidence, *Geol. Soc. Am. Bull.*, *122*, 1951–1968, doi:10.1130/B30108.1.
- Liu, K., A. Levander, Y. Zhai, R. W. Porritt, and R. M. Allen (2012), Asthenospheric flow and lithospheric evolution near the Mendocino Triple Junction, *Earth Planet. Sci. Lett.*, *323–324*, 60–71, doi:10.1016/j.epsl.2012.01.020.
- Manning, C. E. (1994), The solubility of quartz in  $\text{H}_2\text{O}$  in the lower crust and upper mantle, *Geochem. Cosmochem. Acta*, *58*, 4831–4839.
- Manning, C. E. (1996), Effect of sediments on aqueous silica transport in subduction zones, in *Subduction: Top to Bottom*, *Geophys. Monogr.*, vol. 96, edited by G. E. Bebout et al., pp. 277–284, AGU, Washington, D. C.
- Manning, C. E. (1997), Coupled reaction and flow in subductions zones: Si metasomatism in the mantle wedge, in *Fluid Flow and Transport in Rocks*, edited by B. Jamtveit and B. W. D. Yardley, pp. 139–148, Chapman Hall, London.
- McCaffrey, R., A. I. Qamar, R. W. King, R. Wells, G. Khazaradze, C. A. Williams, C. Stevens, J. J. Vollick, and P. C. Zwick (2007), Fault locking, block rotation and crustal deformation in the Pacific Northwest, *Geophys. J. Int.*, *169*, 1315–1340, doi:10.1111/j.1365-246X.2007.03371.x.
- McCaffrey, R., R. W. King, S. J. Payne, and M. Lancaster (2013), Active tectonics of northwestern U.S. from GPS derived surface velocities, *J. Geophys. Res. Solid Earth*, *118*, 709–723, doi:10.1029/2012JB009473.
- McCrorry, P. A., J. L. Blair, F. Waldhauser, and D. H. Oppenheimer (2012), Juan de Fuca slab geometry and its relation to Wadati-Benioff zone seismicity, *J. Geophys. Res.*, *117*, B09306, doi:10.1029/2012JB009407.
- McCrorry, P. A., R. D. Hyndman, and J. L. Blair (2014a), Relationship between the Cascadia fore-arc mantle wedge, nonvolcanic tremor, and the downdip limit of seismogenic rupture, *Geochem. Geophys. Geosyst.*, *15*, 1071–1095, doi:10.1002/2013GC005144.
- McCrorry, P. A., J. E. Constantz, A. G. Hunt, and J. L. Blair (2014b), Helium as a tracer for fluids released from Juan de Fuca lithosphere beneath the Cascadia forearc, Paper 280-6, Geol. Soc. Am. Annual Meeting, Vancouver, Canada, 19–22 Oct. 2014.
- McLennan, S. M., and S. R. Taylor (1996), Heat flow and the chemical composition of continental crust, *J. Geol.*, *104*, 369–377.
- Nadeau, R. M., and D. Dolenc (2005), Nonvolcanic tremors deep beneath the San Andreas Fault, *Science*, *307*, 389–389.
- Nedimović, M. R., R. D. Hyndman, K. Ramachandran, and G. D. Spence (2003), Reflection signature of seismic and aseismic slip on the northern Cascadia subduction interface, *Nature*, *424*, 416–420.
- Obana, K., M. Scherwath, Y. Yamamoto, S. Kodaira, K. Wang, G. Spence, M. Riedel, and H. Kao (2014), Earthquake activity in northern Cascadia subduction zone off Vancouver Island revealed by ocean-bottom seismograph observations, *Bull. Seismol. Soc. Am.*, *104*, doi:10.1785/0120140095.
- Obara, K. (2011), Characteristics and interactions between non-volcanic tremor and related slow earthquakes in the Nankai subduction zone, southwest Japan, *J. Geodyn.*, *52*, 229–248.
- Okazaki, K., I. Katayama, and H. Noda (2013), Shear-induced permeability anisotropy of simulated serpentinite gouge produced by triaxial deformation experiments, *Geophys. Res. Lett.*, *40*, 1290–1294, doi:10.1002/grl.50302.
- Oleskevich, D. A., R. D. Hyndman, and K. Wang (1999), The updip and downdip limits to great subduction earthquakes: Thermal and structural models of Cascadia, south Alaska, SW Japan and Chile, *J. Geophys. Res.*, *104*, 14,965–14,991, doi:10.1029/1999JB900060.
- Peacock, S. M. (1990), Fluid processes in subduction zones, *Science*, *248*, 329–337.
- Peacock, S. M. (1993), Large-scale hydration of the lithosphere above subducting slabs, *Chem. Geol.*, *108*, 49–59.
- Peacock, S. M. (2009), Thermal and metamorphic environment of subduction zone episodic tremor and slip, *J. Geophys. Res.*, *114*, B00A07, doi:10.1029/2008JB005978.
- Peacock, S. M., and R. D. Hyndman (1999), Hydrous minerals in the mantle wedge and the maximum depth of subduction zone earthquakes, *Geophys. Res. Lett.*, *26*, 2517–2520.
- Peacock, S. M., and K. Wang (1999), Seismic consequences of warm versus cool subduction metamorphism: Examples from southwest and northeast Japan, *Science*, *286*, 937–939.
- Peacock, S. M., N. I. Christensen, M. G. Bostock, and P. Audet (2011), High pore pressures and porosity at 35 km depth in the Cascadia subduction zone, *Geology*, *39*, 471–474.
- Phillips, G. N., and R. Powell (2010), Formation of gold deposits: A metamorphic devolatilization model, *J. Metamorph. Geol.*, *28*, 689–718.
- Philpotts, A. R., and J. J. Ague (2009), *Principles of Igneous and Metamorphic Petrology*, 2nd ed., p. 684, Cambridge Univ. Press, New York.
- Ramachandran, K., and R. D. Hyndman (2012), The fate of fluids released from subducting slab in northern Cascadia, *Solid Earth*, *3*, 121–129, doi:10.5194/se-3-121-2012.
- Ranero, C. R., J. P. Morgan, K. McIntosh, and C. Reichert (2003), Bending-related faulting and mantle serpentinization at the Middle America trench, *Nature*, *425*, 367–373.
- Rogers, G., and H. Dragert (2003), Episodic tremor and slip on the Cascadia subduction zone: The chatter of silent slip, *Science*, *300*, 1942–1943, doi:10.1126/science.1084783.
- Royer, A. A., and M. G. Bostock (2013), A comparative study of low frequency earthquake templates in northern Cascadia, *Earth Planet. Sci. Lett.*, *402*, 247–256, doi:10.1016/j.epsl.2013.08.040.

- Rüpke, L. H., J. Phipps Morgan, and H. Connolly (2004), Serpentine and the subduction zone water cycle, *Earth Planet. Sci. Lett.*, *223*, 17–34.
- Scambelluria, M. J., N. Fiebig, O. M. Malaspina, and T. Pettke (2004), Serpentinite subduction: Implications for fluid processes and trace-element recycling, *Int. Geol. Rev.*, *46*, 595–613, doi:10.2747/0020-6814.46.7.595.
- Schmalzle, G. M., R. McCaffrey, and K. C. Creager (2014), Central Cascadia subduction zone creep, *Geochem. Geophys. Geosyst.*, *15*, 1515–1532, doi:10.1002/2013GC005172.
- Schmidt, D. A., and H. Gao (2010), Source parameters and time-dependent slip distributions of slow-slip events on the Cascadia subduction zone from 1998–2008, *J. Geophys. Res.*, *115*, B00A18, doi:10.1029/2008JB006045.
- Schmidt, M. W., and S. Poli (1998), Experimentally based water budgets for dehydrating slabs and consequences for arc magma generation, *Earth Planet. Sci. Lett.*, *163*, 361–379.
- Schmidt, M. W., and S. Poli (2003), Generation of mobile components during subduction of oceanic crust, *Treat. Geochem.*, *3*, 567–591.
- Schwartz, S. Y., and J. M. Rokosky (2007), Slow slip events and seismic tremor at circum-Pacific subduction zones, *Rev. Geophys.*, *45*, RG3004, doi:10.1029/2006RG000208.
- Segall, P., A. M. Rubin, A. M. Bradley, and J. R. Rice (2010), Dilatant strengthening as a mechanism for slow slip events, *J. Geophys. Res.*, *115*, B12305, doi:10.1029/2010JB007449.
- Shelly, D. R. (2010), Migrating tremors illuminate complex deformation beneath the seismogenic San Andreas Fault, *Nature*, *463*, 648–652.
- Shelly, D. R., G. C. Beroza, and S. Ide (2007), Non-volcanic tremor and low-frequency earthquake swarms, *Nature*, *446*, 305–307.
- Sibson, R. H. (1992), Implications of fault-valve behaviour for rupture nucleation and recurrence, *Tectonophysics*, *211*, 283–293.
- Soyer, W., and M. Unsworth (2006), Deep electrical structure of the northern Cascadia (British Columbia, Canada) subduction zone: Implications for the distribution of fluids, *Geology*, *34*, 53–56.
- Szeliga, W., T. Melbourne, M. Santillan, and M. Miller (2008), GPS constraints on 34 slow slip events within the Cascadia subduction zone, 1997–2005, *J. Geophys. Res.*, *113*, B04404, doi:10.1029/2007JB004948.
- van Keken, P. E., B. Kiefer, and S. M. Peacock (2002), High-resolution models of subduction zones: Implications for mineral dehydration reactions and the transport of water into the deep mantle, *Geochem., Geophys., Geosyst.*, *3*, 1–20, doi:10.1029/2001GC000256.
- van Keken, P. E., B. R. Hacker, E. M. Syracuse, and G. A. Abers (2011), Subduction Factory: 4. Depth dependent flux of H<sub>2</sub>O from subducting slabs worldwide, *J. Geophys. Res.*, *116*, doi:10.1029/210/JB007922.
- Wang, K., R. Wells, S. Mazzotti, R. D. Hyndman, and T. Sagiya (2003), A revised dislocation model of interseismic deformation of the Cascadia subduction zone, *J. Geophys. Res.*, *108*, 2026, doi:10.1029/2001JB001227.
- Wang, K., H. Dragert, H. Kao, and E. Roeloffs (2008), Characterizing an “uncharacteristic” ETS event in northern Cascadia, *Geophys. Res. Lett.*, *35*, L15303, doi:10.1029/2008GL034415.
- Wang, K., Y. Hu, and J. He (2012), Deformation cycles of subduction earthquakes in a viscoelastic Earth, *Nature*, *484*, 327–332, doi:10.1038/nature11032.
- Wannamaker, P. E., R. L. Evans, P. A. Bedrosian, M. J. Unsworth, V. Maris, and R. S. McGary (2014), Segmentation of plate coupling, fate of subduction fluids, and modes of arc magmatism in Cascadia, inferred from magnetotelluric resistivity, *Geochem. Geophys. Geosyst.*, *15*, 4230–4253, doi:10.1002/2014GC005509.
- Wech, A. G. (2010), Interactive tremor monitoring, *Seismol. Res. Lett.*, *81*, 664–669, doi:10.1785/gssr181.4.664.
- Wech, A. G., and K. C. Creager (2007), Cascadia tremor polarization evidence for plate interface slip, *Geophys. Res. Lett.*, *34*, L22306, doi:10.1029/2007GL031167.
- Wech, A. G., and K. C. Creager (2008), Automated detection and location of Cascadia tremor, *Geophys. Res. Lett.*, *35*, L20302, doi:10.1029/2008GL035458.
- Wech, A. G., and K. C. Creager (2011), A continuum of stress, strength and slip in the Cascadia subduction zone, *Nat. Geosci.*, *4*, 624–628.
- Wech, A. G., K. C. Creager, and T. I. Melbourne (2009), Seismic and geodetic constraints on Cascadia slow slip, *J. Geophys. Res.*, *114*, B10316, doi:10.1029/2008JB006090.
- Wech, A. G., C. M. Boese, T. A. Stern, and J. Townend (2012), Tectonic tremor and deep slow slip on the Alpine Fault, *Geophys. Res. Lett.*, *39*, doi:10.1029/2012GL051751.
- Williams, M. C., A. M. Tréhu, and J. Braunmiller (2011), Seismicity at the Cascadia plate boundary beneath the Oregon continental shelf, *Bull. Seismol. Soc. Am.*, *101*, 940–950, doi:10.1785/0120100198.
- Worzewski, T., M. Jegen, H. Kopp, H. Brasse, and W. T. Castillo (2011), Magnetotelluric image of the fluid cycle in the Costa Rican subduction zone, *Nat. Geosci.*, *4*, 108–111.
- Zandt, G., and C. J. Ammon (1995), Continental crust composition constrained by measurements of crustal Poisson's Ratio, *Nature*, *374*, 152–154.
- Zhao, D., K. Wang, G. C. Rogers, and S. M. Peacock (2001), Tomographic image of low *P* velocity anomalies above slab in northern Cascadia subduction zone, *Earth Planet Space*, *53*, 285–293.